Reduced Order Modelling of Optimized Heat Exchangers for Maximum Mass-Specific Performance of Airborne ORC Waste Heat Recovery Units

Beltrame, F.; Krempus, D.; Colonna, Piero; de Servi, C.M.

DOI
10.12795/9788447227457_93

Publication date
2024

Document Version
Final published version

Published in
Proceedings of the 7th International Seminar on ORC Power Systems

David Tomás Sánchez Martínez
Lourdes García Rodríguez
(coordinadores)

Proceedings of the 7th International Seminar on

ORC Power Systems

Editorial Universidad de Sevilla

Proceedings of the 7th International Seminar on

ORC Power Systems

David Tomás Sánchez Martínez
Lourdes García Rodríguez
(coordinadores)

Proceedings of the 7th International Seminar on

ORC Power Systems

(ORC2023)

4th to 6th
SEPTEMBER
SEVILLE 2023

EUS EDITORIAL UNIVERSIDAD DE SEVILLA

Sevilla, 2024

Colección Actas
Núm.: 91

ISBN 978-84-472-2745-7
DOI: https://dx.doi.org/10.12795/9788447227457

Diseño de cubierta y maquetación: los autores

INDEX OF CONTRIBUTIONS

ORC SEVILLE 2023
7th International Seminar on O.R.C. Power Systems

DOI: https://dx.doi.org/10.12795/9788447227457_93

REDUCED ORDER MODELLING OF OPTIMIZED HEAT EXCHANGERS FOR MAXIMUM MASS-SPECIFIC PERFORMANCE OF AIRBORNE ORC WASTE HEAT RECOVERY UNITS

Fabio Beltrame[1]*, Dabo Krempus[1], Piero Colonna[1], Carlo De Servi[1,2]

[1] *Delft University of Technology, Propulsion and Power, Aerospace Engineering, Delft, The Netherlands*
[2] *VITO, Thermal Energy Systems, Mol, Belgium*

*Corresponding Author: f.beltrame@tudelft.nl

ABSTRACT

Waste heat recovery (WHR) from aeroengines via compact organic Rankine cycle (ORC) units may increase the fuel efficiency of air transportation. Heat exchangers are arguably the key components of ORC systems for aeronautical applications and their design must be optimized to guarantee the best trade-off between fluid pressure drop, weight and induced aircraft drag. At present, no heat exchangers design guidelines are available for waste heat recovery systems aboard aircraft. This study, thus, contributes to defining a proper design methodology for ORC systems of such applications. The chosen test case is a supercritical ORC system with cyclopentane as the working fluid, which recovers waste heat from the auxiliary power unit of an aircraft. The exhaust gas temperature and mass flow rate of the power unit are known and kept constant in the analysis, and so are the ambient conditions, which define the cold sink of the ORC turbogenerator. Three design strategies targeting minimum mass and maximum net power output of the ORC unit have been assessed. In the first one, the multi-objective optimization is performed by prescribing a priori the geometry and frontal area of the heat exchangers. Thus, only the cycle parameters are optimized. The second method tackles, instead, the simultaneous optimization of the geometric parameters of the condenser and the cycle parameters. It was found that the integrated design allows for system mass reduction by 10 - 12% for a given ORC power output, highlighting the importance of performing the simultaneous optimization of the thermodynamic process and the heat exchanger geometry. Finally, the third method addresses the same optimal design problem by leveraging a reduced-order model of the condenser to predict the optimal design space of this component. The generated Pareto front obtained with this method is very similar to that found by optimizing simultaneously the complete condenser geometry and the cycle parameters. The mean deviation is about 2%. With just one heat exchanger surrogate model, the Pareto front was generated in one fourth of the computational time. This is due to the lower number of optimization variables and the faster objective function evaluation.

1 INTRODUCTION

Research on design of compact heat exchangers (HXs) for aerospace applications has been gaining momentum, being HXs key components of the new technical solutions currently under evaluation to improve the efficiency and sustainability of aircraft propulsion systems. Waste heat recovery (WHR) from aeroengines via compact organic Rankine cycle (ORC) units is, for instance, one of these solutions. The preliminary design of HXs of stationary ORC systems is generally performed once the optimization of the thermodynamic cycle configuration is completed, as the optimal range for the main design specifications of these components, i.e. minimum temperature difference and allowable pressure drops, are known based on a consolidated design practice. In case of mobile systems and especially of aerospace applications, the selection of an appropriate HX topology and the related optimal geometry cannot be decoupled from the design of the thermodynamic cycle, as the fuel savings depend not only on conversion efficiency, which is strongly related to the HXs effectiveness and pressure drops, but also on the overall system weight and limitations on the available space. A consequence thereof is that, currently, there are no specific HX design guidelines for such applications. At present, only a few

studies have documented the integrated design of these components and the thermodynamic process. For instance, Lecompte et al. (2014) optimized the HX geometry together with the ORC WHR system for stationary applications, and highlighted how important it is to optimize these components and choose the right topology to maximize cycle efficiency and minimize costs. Similarly, Chatzopoulu et al. (2019) investigated the off-design performance of a medium power capacity ORC unit recovering heat from stationary internal combustion engines. The subcritical non-recuperated ORC cycle was optimized to maximize net power output during both nominal and off design operations for given characteristics of the HXs and the expander. Two different HX topologies were compared based on the off-design performance map of the various system solutions. In these studies, weight or size constraints were not considered.

Recent research works have also demonstrated that HX optimization is key for the optimum design of aerospace thermal systems. For example, Yu et al. (2016) showed that the optimization of the precooler of an air breathing engine flying at high Mach numbers is needed, not only to achieve system performance improvements, but also to enable the operational feasibility of the engine itself. Ascione et al. (2021) optimized the preliminary design of a vapour compression cycle and its components simultaneously. The results show that the optimum HX dimensions depend on the selected thermodynamic conditions, working fluid, as well as the targeted figure of merit in the design.

In this context, the aim of the present work is to contribute to the development of a computationally efficient methodology to predict the mass-specific performance of optimal HX designs in the early design phase of aerospace thermal systems. Notably, the study explores the development and use of a reduced order model of the HXs to replace the conventional preliminary sizing procedure of these components, and to reduce the degrees of freedom associated to their geometry in the optimization. The selected test case to demonstrate the proposed methodology is a supercritical ORC waste heat recovery unit recovering waste heat from an aircraft auxiliary power unit.

2 TEST CASE

The WHR unit studied in this work consists of an organic Rankine cycle turbogenerator serving as bottoming unit of the auxiliary power unit of an Airbus A320. The process flow diagram of this combined cycle system, named CC-APU, is reported in Figure 1. Cyclopentane is chosen as the working fluid as a previous study indicated that such a fluid is especially suited to gas turbine WHR applications (Krempus et al., 2021). A supercritical ORC configuration is adopted to maximize thermodynamic cycle efficiency. Additionally, for the chosen working fluid and HX materials, the supercritical operating conditions lead to HX designs with wall thicknesses close to the minimum value from a manufacturability standpoint, thus mass savings are arguably limited for lower pressures. The APU characteristics are fixed, together with the ambient pressure and temperature, which corresponds to ISA +25 at 0 m MSL. Only the ORC system design is addressed in this study. The exhaust gases are discharged from the APU at 847.15 K and 1.02 bar with a mass flow rate of 0.87 kg/s.

564

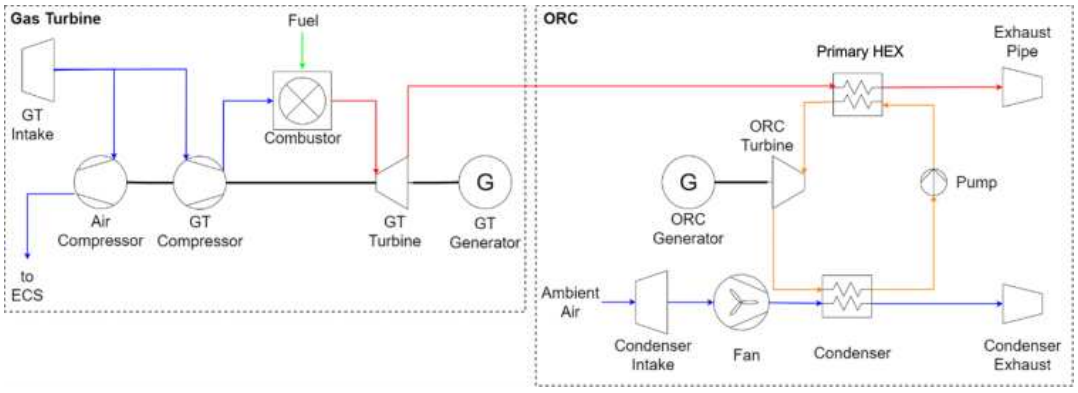

Figure 1: Process flow diagram of the CC-APU system.

3 METHODOLOGY

3.1 ORC system modelling

The performance of the ORC unit is modeled using an in-house tool for on-design thermodynamic cycle calculations. The Helmoltz-energy explicit equation of state (HEOS) implemented in CoolProp (Bell et al., 2014) is used for thermodynamic property modeling of the ORC working fluid. The ideal gas model is, instead, adopted for the APU exhaust gases, whose composition is fixed and assumed to be 74% N2, 15.9% O2, 6.4% CO2, 2.5% H2O, 1.2% Ar (Siebel et al. 2018). Regarding the ORC components, the geometrical characteristics of the primary HX are fixed, while those of the condenser are optimized.

The chosen topology for the primary HX consists in a multi-pass staggered bare-tube bundle where the working fluid circulates inside the tubes, in a counter-crossflow arrangement with respect to the exhaust gases. A nickel-based alloy, HastelloyX, is chosen as the material of the primary HX given the maximum exhaust gas temperature as suggested by Grieb (2004). The tube outer diameter is 1.8 mm, while the tube thickness is calculated given the pressure difference between the working fluid and the exhaust gases. The transverse and longitudinal pitches between the tubes are set to 3 and 1.25 outer diameters, respectively, to minimize the pressure drop and maximize the compactness of the HX, while the number of passes is set to 10. The frontal area is fixed and corresponds to a square of 0.28 x 0.28 meters. These dimensions were chosen considering the size of the APU exhaust duct.

For the ORC condenser, a flat tube microchannel heat exchanger geometry with louvered or offset strip fins is considered. The fin and flat tube thicknesses are set to 0.11 mm and 0.2 mm, respectively, while the height of the microchannels h_{mc} is set to 1.6 mm. The louver fin length L_l was fixed to 85% of the fin height. These values were chosen based on manufacturability considerations. The other geometric parameters highlighted in Table 3 are optimized. The chosen material for the condenser is an aluminum alloy of the 3000 series, as suggested in the technical report by Kaltra Gmbh (2020).

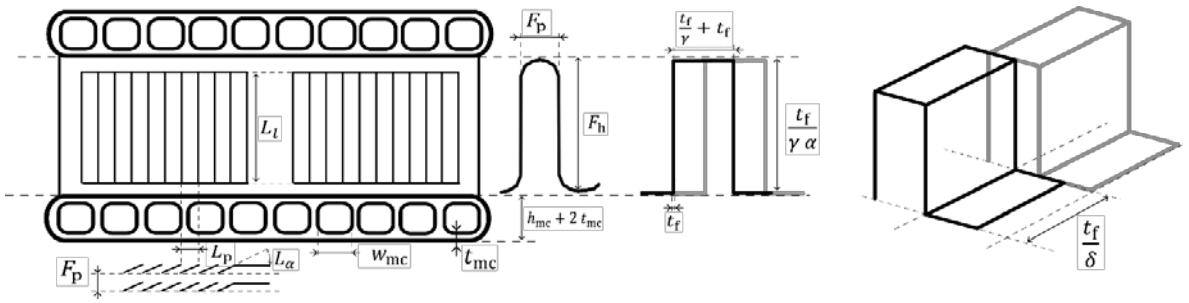

Figure 2: Sketch of the flat tube microchannel with louver or offset strip fins geometry.

The turbine power output $\dot{W}_{\mathrm{turb}}$ is calculated assuming a constant isentropic efficiency of 0.94, a mechanical efficiency of 0.99, and a generator efficiency of 0.97. The working fluid is pressurized by a centrifugal pump, while an electrically driven fan provides the necessary air mass flow rate $\dot{m}_{\mathrm{air}}$ to the condenser. The net power output of the WHR unit is thus calculated by subtracting the fan and pump power consumptions to the turbine power, see Equation (2). The isentropic fan and pump efficiencies are assumed equal to $\eta_{\mathrm{is,f}} = 0.6$ and $\eta_{\mathrm{is,p}} = 0.65$, respectively, while the mechanical and conversion efficiencies are fixed to $\eta_{\mathrm{m,f}} = \eta_{\mathrm{m,p}} = 0.98$.

$$\dot{W}_{\mathrm{net}} = \dot{W}_{\mathrm{turb}} - \frac{\dot{m}_{\mathrm{air}} \Delta P_{\mathrm{air}}}{\rho_{\mathrm{air}} \eta_{\mathrm{is,f}}\, \eta_{\mathrm{m,f}}} - \frac{\dot{m}_{\mathrm{wf}}\, \Delta H_{\mathrm{p}}}{\eta_{\mathrm{is,p}}\ \eta_{\mathrm{m,p}}} \tag{1}$$

The ORC system mass M_{ORC} is estimated as the sum of the mass of the main ORC system components (pump, turbogenerator, condenser, primary HX, fan), of the working fluid, and of the balance-of-plant. The HX mass is an outcome of the respective sizing models, see the following section. Assuming that the primary HX is fully flooded at the start-up, the working fluid mass is estimated as the primary HX cold side volume augmented by 20% to account for system piping, times the fluid density at standard ambient conditions. The turbo-generator mass is estimated assuming a specific power of around 5.5 kW/kg, based on the results in Geest et al. (2015). The same approach is adopted for the centrifugal pump, whose specific power is assumed to be 4 kW/kg as reported by Kwak et al. (2018). The mass of

the fan including its motor and that of the balance-of-plant are assumed to contribute 10% to the overall system mass. Note also that the sizing of the equipment and the weight estimation are performed once the thermodynamic cycle calculations are completed.

3.2 Heat exchanger sizing

The required size of the HX varies depending on the cycle specifications. The HX models thus consist of a sizing procedure aimed at finding the heat transfer area A_{ht} that satisfies the required heat duty given the inlet temperature, pressure, and mass flow rate of the hot and cold streams. For this task, in-house tools have been developed in python and verified using the software EchTherm. The output of the sizing procedure includes the HX dimensions, mass, and pressure drops on the cold and hot sides. For both the heat exchangers of the ORC unit, the height *Y* and width *X* on the gas side, which determine the frontal area, are an input to the design routine. The heat exchanger depth *Z* is instead calculated to meet the design specifications. In the case of the condenser, this corresponds to determining the number of microchannels n_{mc} of width w_{mc} within the flat tubes, while for the primary HXs the dependent variable is the number of streamwise tubes per pass n_{z}. As fluid properties can change significantly on the working fluid side, in both the condenser and the primary HX models, the geometry is discretized in several control volumes, or cells, in which mean properties are estimated. As the primary HX features multiple fluid passes, the number of cells is set conveniently equal to the number of passes, which is an input of the design problem. For the condenser, the number of cells, or control volumes, is set equal to three, one for each thermodynamic region involved in the condensation process of the fluid (superheated vapour, two-phase fluid, and subcooled liquid). These control volumes encompass a portion of the flow path of both the working fluid and of the air or exhaust gas streams, but they differ in size, due to the different enthalpy drop $\Delta H_{\mathrm{H}}^{i}$ associated with the thermodynamic state. This quantity as well as the pressure drops are estimated by implementing different empirical correlations, depending on the geometry and fluid phase. The heat transfer correlations are formulated in terms of Colburn factor or Nusselt number, while the pressure drop calculation is based on the estimate of the friction factor or the pressure gradient dP/dz. Table 1 lists the set of correlations implemented in the HXs models. The code solves the equations of the model by determining iteratively the heat transfer area A_{ht}^{i} of each control volume or cell *i* as

$$A_{\mathrm{ht}}^{i} = \frac{\dot{m}\,\Delta H^{\mathrm{i}}}{F^{i}\,\Delta T_{\mathrm{ml}}^{i}\,U^{i}}, \tag{2}$$

where U^{i} is the local overall heat transfer coefficient, $\Delta T_{\mathrm{ml}}^{i}$ is the local mean logarithmic temperature difference, and F^{i} is its correction factor, which is lower than unity for non-constant temperature heat transfer and any flow arrangement different from pure counterflow. The design routine stops when the relative difference in the estimated overall heat transfer area between two consecutive iterations is smaller than 1%.

Table 1: List of correlation used in the heat exchanger models.

HX	Fluid	Property	Reference
Primary HX	Exhaust gas (Tube bundle)	Nu f	Leveque analogy, Shah (2003) VDI (2010, Ch. L1)
Condenser	Air (Louvered fins)	j f	Chang and Wang (1997) Chang et al. (2000)
Condenser	Air (Offset strip fins)	j, f	Manglik and Bergles (1995)
Condenser / Primary HX	WF – single phase	Nu f	Taler (2017) Colebrook-White (VDI, Ch. L1, 2010)
Condenser / Primary HX	WF – two-phase (Condensation)	$\mathrm{d}P/\mathrm{d}Z$ h_c	Müller-Steinhagen and Heck (1986) Shah (2019)

3.3 ORC system design strategies

Three strategies are investigated in this work to design the ORC WHR unit. In the first one, only the thermodynamic cycle parameters are optimized. The degrees of freedom associated with the ORC configuration are the maximum and minimum working fluid temperatures, the maximum cycle pressure, as well as the evaporator and the condenser pinch point temperature differences. Table 2 lists for these variables the considered bounds in the optimization. The second design strategy deals with the simultaneous optimization of the thermodynamic cycle parameters and the condenser geometry. The design variables associated with this component vary depending on the selected fin topology, which can be of the offset strip or louvered type. In both cases, the width of the microchannels within the flat tubes, w_{mc} , is one of the degrees of freedom of the design problem. The total number of design variables is 9 in the case the condenser features offset strip fins, and 10 in the case of louvered fins. Table 3 reports the lower and upper bounds of all the optimization variables related to the condenser geometry. For more details about the parametrization of the fin shapes, the reader is referred to Chang and Wang (1997) for the louvered fins, and to Manglik and Bergles (1995) for the offset strip fins.

Table 2: ORC WHR design parameters and corresponding bounds in the optimization

Parameter	$T_{min,ORC}$ [K]	$T_{max,ORC}$ [K]	$P_{max,ORC}$ [bar]	$\Delta T_{pp,evap}$ [K]	$\Delta T_{pp,cond}$ [K]
Min	367	517.12	47.4	10	10
Max	378	547.84	67.7	50	50

Table 3: Bounds of the optimization variables related to the condenser geometry.

Geometry	Channels	Louvered fins				Offset strip fins		
Parameter	w_{mc} (mm)	F_{h}(mm)	F_{p}(mm)	L_{α} (°)	L_{p}(mm)	α (-)	δ (-)	γ (-)
Min	1	6	0.9	10	0.9	0.1	0.012	0.038
Max	2.5	16	3	30	3	1	0.037	0.122

The third design strategy relies on a reduced-order model of the condenser. This is calibrated by first optimizing the condenser geometry, either featuring offset-strip or louvered fins, for a set of process conditions, by using the same model used for the sizing. The optimization results are then exploited to define a surrogate model representing the optimal design space of the condenser, which is then used to replace the original condenser model when solving the optimal design problem of the ORC unit. The advantage is a drastic reduction in the computational cost of the system optimization. Notably, the number of design variables reduces from 9 or 10, depending on the condenser geometry, to 6.

As for the optimization algorithm, the NSGA-II routine (Deb et al., 2002) is used. Notably, the objective functions considered in the ORC WHR unit preliminary design are the minimization of the system mass M_{ORC} and the maximization of the net power output $\dot{W}_{\mathrm{net}}$. The manipulated variables are the cycle parameters in Table 2 and the condenser design variables in Table 3, depending on the selected fin geometry. If the surrogate model is adopted, the optimization variables associated to the condenser geometry reduces to only one, as explained in Section 3.4. The optimization problem related to the preliminary design of the ORC unit can thus be stated as follows:

$$\begin{aligned} &\text{Minimize:} && M_{ORC}\,, -W_{\mathrm{net}} \\ &\text{Subject to:} && Z_{\mathrm{min}} \leq Z_{HX} \leq Z_{\mathrm{max}} \\ & && \Delta P_{wf} \leq 3\%\ \mathrm{P_{wf,in}}. \end{aligned}$$

3.4 Reduced order model for the optimal condenser design

The proposed reducer-order modeling strategy for the ORC condenser begins with the generation of a dataset of optimal condenser solutions for a set of process conditions. Notably, for a given fin topology, the condenser geometry is optimized with respect to two objective functions, which are the minimization of the HX mass and the air pressure drop. The NSGA-II is again employed to optimize the two objectives simultaneously, by varying the geometry degrees of freedom while satisfying specific

constraints on the size of the HX and the working fluid side pressure drop. The output of the multi-objective optimization is a set of Pareto-optimal solutions for each process condition. The optimization problem can thus be stated as follows:

$$\begin{aligned} &\text{Minimize:} && M_{\mathrm{HX}}\,, \Delta P_{\mathrm{air}} \\ &\text{Subject to:} && Z_{\min} \le Z_{\mathrm{HX}} \le Z_{\max} \\ & && \Delta P_{\mathrm{wf}} \le 3\%\ \mathrm{P}_{\mathrm{wf,in}}. \end{aligned}$$

Four process conditions fully specify the design point of the condenser, namely the cooling air and fluid mass flow rates ($\dot{m}_{\mathrm{air}}, \dot{m}_{\mathrm{wf}}$), the condensation pressure p_{cnd} and de-superheating degree, which is defined as $\Delta T_{\mathrm{dsh}} = T_{\mathrm{wf,in}} - T_{\mathrm{cnd}}$. To extend the reduced order model validity, the air inlet temperature $T_{\mathrm{air,in}}$ is also varied. The range considered for these variables, which determine the validity range of the reduced order model, are reported in Table 4. The corresponding condenser heat duty varies from 256 to 388 kW. The upper and lower bounds of Table 4 are defined by analyzing the solutions resulting from the simultaneous optimization of the thermodynamic cycle specifications and the condenser geometry, indicated as optimization strategy #1 in Section 3.3.

Table 4: Range of process conditions for the generation of the condenser optimal design dataset.

	$\dot{m}_{air}$	$\dot{m}_{wf}$	p_{cnd}	ΔT_{dsh}	$T_{air,in}$
Min	7.25 kg/s	0.68 kg/s	3.58 bar	10 K	305.6 K
max	9.25 kg/s	0.85 kg/s	4.76 bar	60 K	316.0 K

The next step of the procedure in the definition of the reduced-order model is data reduction. Let a specific Pareto front be represented by a basis function shared by the whole dataset. This basis function is defined by a small set of coefficients that need to be calculated for each curve, and a validity interval. By nondimensionalizing the heat exchanger mass and pressure drop as $\widetilde{M}_{\mathrm{HX}} = M_{\mathrm{HX}}/(A_{\mathrm{fr}}\,\rho_{\mathrm{mat}}\,l_{\mathrm{ref}})$ and $\widetilde{\Delta P}_{\mathrm{air}} = \Delta P_{\mathrm{air}}\ A_{\mathrm{fr}}^2\,\rho_{\mathrm{air,in}}\,\dot{m}_{\mathrm{air}}^{-2}$, where l_{ref} is the flat tube height, $\rho_{\mathrm{air,in}}$ is the density of the cold air before entering the core, ρ_{mat} is the material density of the HX and A_{fr} is its frontal area, the basis function

$$\phi(x) = w_0 + \left(\frac{x}{w_1}\right)^{w_2} \tag{3}$$

with the Pareto front-specific fit coefficients w_0, w_1, w_2 can reliably and accurately fit the whole database. The fit coefficients $w^* = [w_0, w_1, w_2]$ for each Pareto front are the result of a gradient based optimization that minimizes the coefficient of determination R^2 of equation (3) with respect to the points on the Pareto front. The optimization is performed using the *minimize* function of the *Scipy* pacakage with the SLSQP solver (Kraft, 1988). The mean standard uncertainties on the three fit coefficients for the whole dataset are 2.3%, 0.9% and 3.7%.

The next step is to determine the range of validity of each Pareto front representation. The nondimensional pressure drop $\widetilde{\Delta P}_{\mathrm{air}}$ is the Euler number with respect to the inlet conditions of the cooling air. The minimum Euler number Eu_m, which is the first point of the Pareto front, proves to be an optimal choice as the predictor for the validity range. The reason thereof is that Eu_{m} follows a quasi-linear trend with respect to the five process variables varied to generate the database. These linear trends can, then, be superimposed to predict the minimum Euler number as

$$Eu_{\mathrm{m}} = Eu_{\mathrm{m_0}} + \frac{\partial Eu_{\mathrm{m}}}{\partial\, \dot{m}_{\mathrm{air}}}\Delta\, \dot{m}_{\mathrm{air}} + \frac{\partial Eu_{\mathrm{m}}}{\partial\, \dot{m}_{\mathrm{wf}}}\Delta\, \dot{m}_{\mathrm{wf}} + \frac{\partial Eu_{\mathrm{m}}}{\partial\, T_{\mathrm{cnd}}}\Delta\, T_{\mathrm{cnd}} + \frac{\partial Eu_{\mathrm{m}}}{\partial\, \Delta T_{\mathrm{dsh}}}\Delta\, \Delta T_{\mathrm{dsh}} + \frac{\partial Eu_{\mathrm{m}}}{\partial\, T_{\mathrm{c,in,cond}}}\Delta\, T_{\mathrm{c,in,cond}}\,, \tag{4}$$

where Δ expresses the difference between the value of a given process variable and the corresponding lower bound in Table (4). The derivatives of the minimum Euler number with respect to each thermodynamic variable v^i are numerically calculated over the dataset as

$$\frac{\partial Eu_{\mathrm{m}}}{\partial\, v^i} = \frac{1}{N_{TC}}\sum_{j=0}^{N_{TC}} \frac{1}{N_{step}^j}\sum_{k=0}^{N_{step}^j}\left(\frac{\Delta Eu_{\mathrm{m}}(j,k)}{\Delta v^i(j,k)}\right). \tag{5}$$

The mean relative error and its standard deviation on the whole database between the predicted value f Eu_{m} using equation (4), and the original values of the Pareto fronts is 3.8% and 8.1 % for the louvered fins, and 3.1% and 10% for the offset strip fins. Figure 3 compares the fitted basis-function predictions with the Pareto front solutions for five exemplary process variable sets. Notice that the curves start from the predicted minimum Euler number, which is highlighted as a red star in the figure.

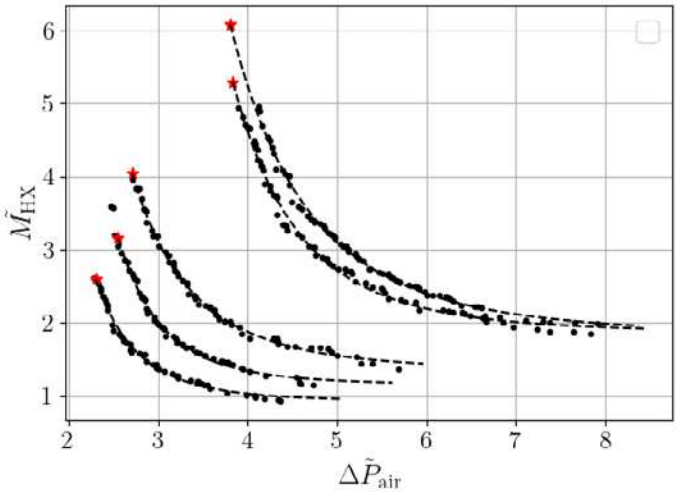

Figure 3: Pareto front fits for five different process conditions - Louvered fin condenser.

The final step of the calibration of the reduced order model is the prediction of the coefficients w^* as a function of the process conditions. A multi-output linear regression model is chosen for this task. The range of the process variables, as well as of the calculated coefficients w^*, is rescaled to (0,1) to properly train the regression model, whose weights are estimated using an ordinary least squares algorithm (Lawson, 1987).

569

The reduced order model of the condenser consists of a function implemented in python language which uses the linear regression model and the coefficients of equation (4) determined for each HX topology to predict the coefficients w^* of ϕ and the minimum Euler number of the Pareto front, given as input the process variables of interest, the heat exchanger frontal area, and material density. By means of the reduced-order model, the degrees of freedom associated to the condenser design reduce to only one: the ratio of the Euler number over the minimum Euler number $Eu^* = Eu/Eu_m$ of the reconstructed basis function. As the range of variation of Eu^* is almost the same for all the Pareto curves of the database, Eu^* can be used as optimization variable. The fact that the maximum value of Eu^* of the Pareto curves varies between 1.8 and 2.5, does not pose a problem to the optimization, as all the curves tend to flatten out in correspondence of their maximum value of Euler number, and this asymptotic trend is captured by the basis-functions.

Thus, the input of the reduced-order model during a system optimization consist of a set of process variables, the Eu^* and the choice of the fin topology. The output, instead, includes the air side pressure drop and the minimum mass of the optimal HX. Note that the working fluid side pressure drop is not predicted by the reduced order model, and it is then assumed constant when estimating the ORC unit performance. Notably, its value is taken equal to upper bound considered for this quantity in the generation of the dataset of optimal condenser geometries, see Section 3.4. This introduces a small error in the system optimization since the working fluid pressure drop does not vary significantly over the optimal design space of the condenser. If during the system optimization the input process conditions exceed the bounds defined in the training dataset, see Table 4, the surrogate model returns a warning, and its prediction can be discarded.

4 RESULTS

The developed simulation and optimization infrastructure has been used i) to investigate for an ORC WHR unit aboard an aircraft the design improvements achievable by optimizing simultaneously the HX geometry and thermodynamic cycle characteristics, ii) to compare, for the same application, two ORC

condenser topologies, namely the flat tube microchannel with either louvered or offset strip fins, in terms of minimum weight and air pressure drop, and iii) to demonstrate the effectiveness of the proposed reduced-order modelling technique for the preliminary design of HXs of aerospace thermal systems.

4.1 Simultaneous optimization of thermodynamic cycle and heat exchanger geometry

To estimate the improvements achievable through the simultaneous optimization of the thermodynamic cycle and heat exchanger preliminary design for the application at hand, the results found via the proposed methodology are compared with those obtained when only thermodynamic cycle optimization is performed, see Figure 4. In this second case, the condenser geometry is fixed by randomly choosing one of the Pareto fronts of the dataset generated for the calibration of the condenser reduced-order model. The geometry is then taken equal to that of the solution located at the center of the chosen Pareto front and kept constant throughout the system optimization.

Several conclusions can be drawn. First, less solutions are found if the condenser geometry is kept constant, regardless of the chosen thermodynamic cycle specifications. This is to be expected, as the geometry cannot be adapted to comply with the different design conditions. Second, the overall system weight decreases by about 12% for the offset strip fins and 10% for the louvered fins for a given net power output of the ORC unit when the thermodynamic cycle specifications and condenser geometry are optimized simultaneously. Third, the condenser with offset strip fins tends to be lighter if low pressure drops are targeted, thus allowing for higher net power outputs. However, the solutions with the louvered fins can yield lighter designs at the costs of larger pressure drops. It follows that depending on the chosen net power output of the ORC system, the optimal HX topology changes, as the two Pareto curves cross each other. In the case of fixed condenser geometry, this crossing point is located at a net power output of 71 kW. If the condenser geometry is optimized together with the thermodynamic cycle, the crossing point shifts to 64 kW, showing that for the chosen test case, the offset strip fins have a larger range of applicability with respect to the louvered fins. The gains in terms of power density achieved by tuning the condenser geometry are significant: if the geometry is kept fixed, the ORC WHR power density ranges from 1.13 to 1.57 kW/kg in the case of offset strip fins, and from 1.09 to 1.67 kW/kg in the case of louvered fins. When the geometry is optimized together with the thermodynamic cycle conditions, the power density range is extended to 1.01 - 1.78 kW/kg for the offset strip fins, and to 1.02 - 1.84 kW/kg for the louvered fins. These results show that the optimization of HX geometry together with the cycle parameters, although computationally more expensive, yields significant performance improvements with respect to fixing a priori the geometry.

570

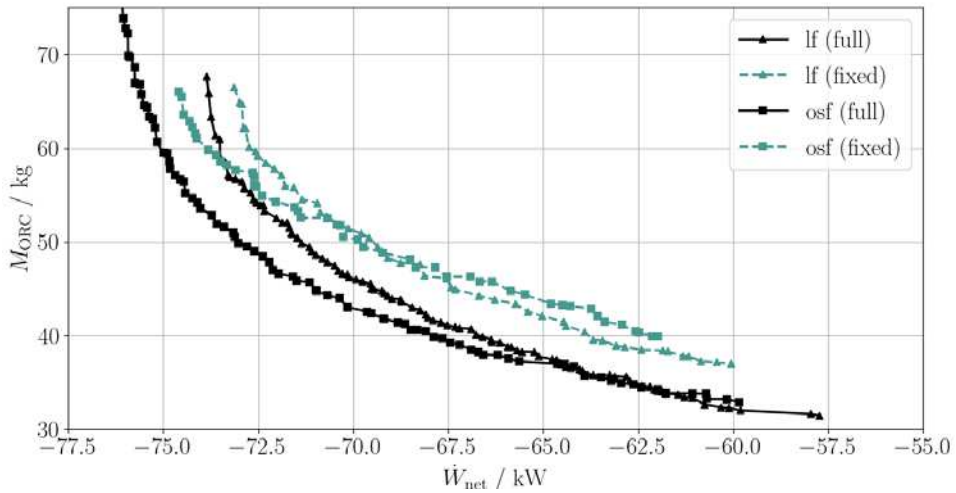

Figure 4: Pareto front of the optimal ORC WHR unit design when the condenser geometry is optimized (full) or when is fixed regardless of the thermodynamic cycle specifications (fixed).

4.2 System design optimization with the optimal HX reduced order model

Figure 5 compares the results of the system optimization obtained using the condenser reduced order model (ROM) with those corresponding to the simultaneous optimization of the thermodynamic cycle

specifications and of the full condenser geometry, for both the louvered fin (a) and offset strip fin (b) cases. The results of the optimization with the condenser ROM match reasonably well those obtained with the original system model for both fin types. Taking the solution of the original system model as reference, the mean relative error between the two set of results is 1.9% for the louvered fin HX (Figure 5a) with a standard deviation of 1.2%, while is 2.4% for the offset strip fin case (Figure 5b) with a standard deviation of 1.4%. Though the Pareto fronts predicted with the two methods are similar, the maximum net power output resulting from the optimization with the condenser ROM tends to be smaller. This can be attributed to i) the limited set of process conditions considered while generating the database used to fit the ROM, and ii) to an underestimation of the minimum Euler number, as high net power outputs are predicted in correspondence of low pressure drops across the condenser. The method adopted to predict the minimum Euler number must then be improved, as the assumption of a linear variation of this quantity with the individual process variables only holds for relatively small variations of the process conditions.

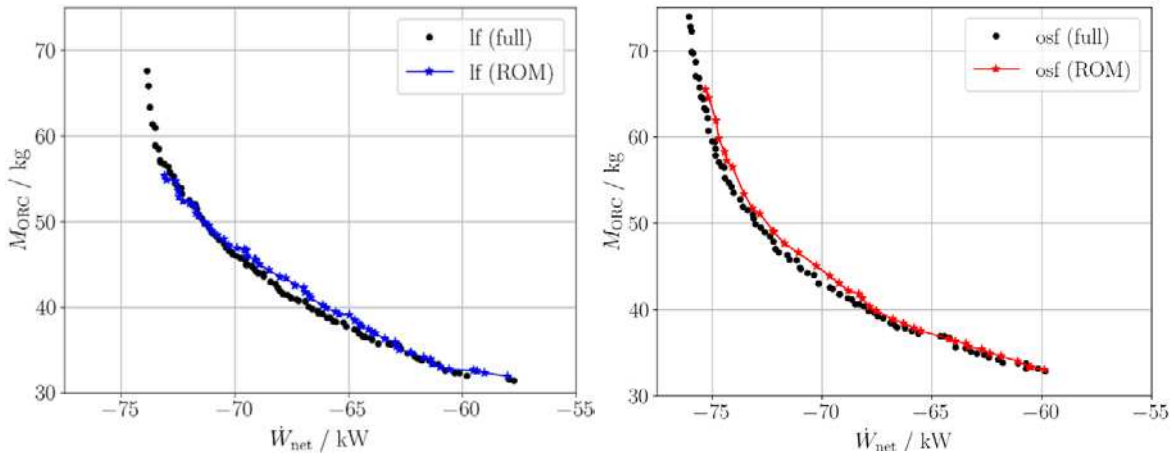

Figure 5: Pareto fronts of the ORC WHR unit optimal designs determined by using the condenser reduced order model (ROM) and by optimizing the HX geometry (full), for both the louvered fin (a) and offset strip fin (b) topologies.

Table 5 compares the computational costs[1] of the three optimization strategies described in Section 3.3. The first one tackles the optimization of the sole thermodynamic cycle design variables, while the HX geometry is fixed. The second and third strategies deal with the simultaneous optimization of both the cycle and condenser design, using the HX sizing procedure of Section 3.2 (strategy #2), or the condenser reduced-order model (strategy #3).

Table 5: Computational performance of the three design optimization strategies

Optimization strategies	Time (min)	pop X gen	Time per iteration
#1	13-14	50 x 50	0.34 s
#2	58-60	96 x 100	0.38 s
#3	15-16	60 x 56	0.29 s

The reduction in computational cost of the system optimization using the ROM is significant, even though this replaces only one HX model. There are two main factors contributing to the reduction of computational time. First and foremost, the optimization problem dimensionality is reduced: the number of optimization variables decreases, together with the population size and number of generations of the genetic algorithm to reach convergence (Pareto optimal solutions invariant for more than 5 generations). The number of function evaluations goes from 9600 to 3360. Secondly, the time per objective function evaluation decreases, as the ROM is about 200 times faster than the condenser sizing model. As a result,

[1] Optimizations were performed on 8 cores, with an AMD Ryzen 4000 series processor.

the average computational time for objective function evaluation using the ROM is reduced by about 25%.

5 CONCLUSIONS

The present work contributes to the development of a design methodology for airborne ORC systems, whose performance is highly dependent on the preliminary design of HXs, as demonstrated in Section 4.1. The following conclusions are drawn from the study:

I) To identify the optimal design of an aerospace ORC unit in terms of efficiency and weight, the optimization of the thermodynamic cycle and the preliminary design of the HXs must be integrated. The performance gains achievable with the integrated optimization vary depending on the HX topology. The microchannel condenser equipped with offset strip fins features a lower weight than in the case of louvered fins, though the latter allows for lighter designs if higher pressure drops are accepted.

II) The outlined methodology to construct a surrogate model of the optimal design space of a HX has proven to be valid: the Pareto front of the optimal solutions for the ORC application at hand predicted when the condenser ROM is used differ from that obtained with the original system model by less than 2%. The accuracy of the reduced order model depends on the size and resolution of the dataset used to fit the model, as well as on the method adopted for the prediction of the minimum Euler number.

III) The use of a ROM for HXs preliminary design significantly reduces the computational cost associated with the integrated optimization of a thermodynamic cycle and its components, at the expense of a small margin of uncertainty. Anyhow, this margin of error is smaller than the benefit achievable with integrated cycle and HX optimization. As the ROM methodology is applied to more HXs, the computational time is expected to decrease significantly.

NOMENCLATURE

A_{fr}	frontal area	(m^2)
A_{ht}	HX heat transfer area	(m^2)
ΔP	pressure drop across the HX	(Pa)
Eu	Euler number	(-)
f	friction factor	(-)
F	correction factor	(-)
F_{h}	fin height	(mm)
F_{p}	fin pitch	(mm)
H	Enthalpy	(J/kg)
j	Colburn factor	(-)
L_α	louver fin angle	(°)
L_{p}	louver pitch	()
M	mass	(kg)
$\dot{m}$	mass flow rate	(kg/s)
n_{mc}	number of microchannels	(-)
n_z	number of streamwise tubes	(-)
p	pressure	(bar)
T	temperature	(K)
t_{f}	fin thickness	(mm)
t_{mc}	microchannel thickness	(mm)
U	global heat transfer coefficient	(W/(m^2 K))
$\dot{W}$	mechanical power	(W)
w_{mc}	microchannel width	(mm)
X	HX width	(m)
Y	HX height	(m)
Z	HX depth	(m)

Greek symbols

α	fin width over height	(-)
γ	fin thickness over depth	(-)
δ	fin thickness over width	(-)
η	efficiency	(-)
ρ	density	(kg/m^3)
ϕ	basis function	(-)

Subscript

air	cold air side
cond	condenser
cnd	condensation conditions
evap	evaporator
f	fan
in	HX inlet conditions
is	isentropic
p	pump
pp	pinch point
wf	working fluid side

REFERENCES

Ascione, F., De Servi, C.M, Colonna, P., 2021, 'Assessment of an inverse organic rankine cycle system for the ECS of a large rotorcraft adopting a high-speed centrifugal compressor and a low GWP refrigerant', ORC Conference, id 110.

Bell, I. H., Wronski, J., Quoilin, S. and Lemort, V., 2014, 'Pure and pseudo-pure fluid thermophysical property evaluation and the open-source thermophysical property library Coolprop', Industrial & Engineering Chemistry Research 53(6), 2498–2508.

Chang, Y., Hsu, K., Lin, Y. and Wang, C., 2000, 'A generalized friction correlation for louver fin geometry', International Journal of Heat and Mass Transfer.

Chang, Y. and Wang, C., 1997, 'A generalized heat transfer correlation for louver fin geometry', International Journal of Heat and Mass Transfer.

Chatzopoulou, M.A., Lecompte, S., De Paepe, M., Markides, C. N., 2019, 'Off-design optimisation of organic Rankine cycle (ORC) engines with different heat exchangers and volumetric expanders in waste heat recovery applications', Applied Energy, Vol 253.

Colonna, P. and van der Stelt, T., 2019, 'Fluidprop (version 3.1): A program for the estimation of thermophysical properties of fluids'.

Deb, K., Pratap, A., Agarwal, S., and Meyarivan, T., 2002, "A Fast and Elitist Multi-Objective Genetic Algorithm: NSGA-II," IEEE Transactions on Evolutionary Computation, Vol. 6, No. 2.

Grieb, H., 2004, "Projektierung von Turboflugtriebwerken", Birkhäuser Basel.

Kaltra GmbH (2020), Microchannel condensers: heat exchangers for condenser applications, technical report, URL https://www.kaltra.com/wp-content/uploads/2020/04/TM_Microchannel-Condensers_Ver.3.0_EN.pdf

Krempus, D., Bahamonde, S., Stelt, T. V. D., De Servi, C. M., Klink, W. and Colonna, P.,2021, 'On Mixtures as Working Fluids for Air-cooled ORC Bottoming Power Plants of Gas Turbines', ORC Conference, id 68.

Kraft, D., 1988, "A software package for sequential quadratic programming", Tech. Rep. DFVLR-FB 88-28, DLR German Aerospace Center – Institute for Flight Mechanics, Koln, Germany.

Kwak, H. D., Kwon, S. and Choi, C. H. (2018), 'Performance Assessment of Electrically Driven Pump-fed LOX/Kerosene Cycle Rocket Engine: Comparison with Gas Generator Cycle', Aerospace Science and Technology 77, 67–82.

Lawson C., Hanson R.J., 1987, 'Solving Least Squares Problems', SIAM

Lecompte, S., Van den Broek, M., De Paepe, M., 2014, "Optimal selection and sizing of heat exchangers for organic rankine cycles (ORC) based on thermo-economics" Proceedings of the 15th International heat Transfer Conference, 7381-7394.

Manglik, R. M. and Bergles, A. E., 1995, "Heat Transfer and Pressure Drop Correlations for the Rectangular Offset Strip Fin Compact Heat Exchanger," Experimental Thermal and Fluid Science, Vol. 10, No. 2, pp. 171-180.

Müller-Steinhagen, H. and Heck, K., 1986, 'A simple friction pressure drop correlation for two-phase flow in pipes', Chem. Eng. Process Intensification 20(6), 297–308.

Shah, R. Sekulic, D. (2003), Fundamentals of heat exchanger design, John Wiley and Sons.

Shah, M., 2019, 'Improved Correlation for Heat Transfer during Condensation in Conventional and mini/micro-channels', Int. Journal of Refrigeration.

Siebel, T., Zanger, j., Huber, A., Aigner, M., Knobloch, K., Bake, f:, 2018, 'Experimental Investigation of Cycle Properties Noise and Air Pollutant Emissions of an APS3200 Auxiliary Power Unit', Journal of Engineering for Gas Turbines and Power, ASME.

Yu, S., Jones, S., Ogawa, H., Karwa, N., 2016, 'Multi-Objective Design Optimization of Precoolers for Hypersonic Airbreathing Propulsion', Journal of Thermophysics and Heat Transfer, 31, 1-13.

VDI e. V. (2010), VDI Heat Atlas, 2nd edition, Springer.

This book contains the compilation of works contributed to the *7th International Seminar on Organic Rankine Cycle Power Systems* (ORC 2023), held in Seville between the 4th and 6th of September 2023. The event was hosted by Universidad de Sevilla on behalf of the Knowledge Centre on Organic Rankine Cycle Technology (KCORC), incorporated in The Netherlands.

The ORC conference, organized biennially, stems as the only conference that is specific to ORC technology, therefore gathering a diverse community whose affiliation spans across all the interested stakeholders, not only in this particular technology but also and in a broader context, in the energy transition. Original equipment manufacturers, professional associations, end-users, investors, policy makers, academics, scientists feel at home at ORC 2023.

The almost 100 proceedings in this book cover a wide variety of topics, from fundamentals to system integration through component design, accounting for thermodynamic performance as well as component design. In addition to this, and as a new track in 2023, works on heat pump technology were also accepted in order to raise awareness of the strong ties between both technologies, specifically in energy storage applications.

This book provides an excellent overview of the current maturity of power systems based on Organic Rankine Cycle technology for applications as diverse as geothermal and waste heat recovery in industry or downstream of other prime movers (e.g., marine applications). It is also an excellent source of information to understand the current challenges faced by the technology, stemming from a very competitive market and increasingly stringent environmental regulations.

The organizers of ORC 2023 hope that the reader finds this work as exciting as the attendees to the conference and, maybe, make the decision to join the 8th edition to the conference in 2025.

KCORC
KNOWLEDGE CENTER
ORGANIC RANKINE CYCLE

eus EDITORIAL
UNIVERSIDAD DE SEVILLA